Exactly self-similar left-sided multifractal measures

Benoit B. Mandelbrot
Department of Physics, IBM Thomas J. Watson Research Center, Yorktown Heights, New York 10598
and Department of Mathematics, Yale University,
Box 2155 Yale Station, New Haven, Connecticut 06520

Carl J. G. Evertsz and Yoshinori Hayakawa*
Department of Applied Physics, Yale University,
Box 2155 Yale Station, New Haven, Connecticut 06520
(Received 12 April 1990)

We introduce and investigate a family of exactly self-similar nonrandom fractal measures, each having stretched exponentially decreasing minimum probabilities. This implies that $\tau(q)$ is not defined for $q<0$ and that $q_{\text{bottom}}=0$ is a critical value of q. Since the partition function does not scale for all values of q, these measures are not multifractals in the restricted sense due to Frisch and Parisi [in *Turbulence and Predictability of Geophysical Flows and Climate Dynamics,* Proceedings of the Enrico Fermi International School of Physics, edited by M. Ghil, R. Benzi, and G. Parisi (North-Holland, New York, 1985), p. 84] and to Halsey *et al.* [Phys. Rev. A **33**, 1141 (1986)]. However, they are exactly self-similar, hence are multifractals in a much earlier and more general meaning of this notion [B. Mandelbrot, J. Fluid Mech. **62**, 331 (1974)]. We show that in these measures the "free energy" $\tau(q)$ is singular at $q=q_{\text{bottom}}$, in the sense that $\tau(q)=-1+c_\lambda q^\lambda+c_1 q+c_2 q^2+O(q^3)$, where $0<\lambda$ is a "critical" exponent. For $\lambda\le 1$, the transition in the $f(\alpha)$ is smooth (i.e., of infinite order), while for $\lambda>1$, the transition order is ≥ 2. We then use a new sampling method to study problems arising in the study of such transitions in case of undersampling.

I. INTRODUCTION

Although at one time the distinction seemed to lack practical application, we feel that recent work on fully developed turbulence and on diffusion-limited aggregation (DLA) has made it essential to distinguish between at least two meanings of the term "multifractal." The more general meaning comes from the notion of "*multiplicative cascade* that generates random measures" and refers to such "multiplicatively generated measures." The virtue of all multiplicatively generated measures is that they are exactly renormalizable or self-similar, just like the simplest self-similar fractals, such as the Sierpiński gasket. This general meaning has been investigated in early[1–4] and recent papers[5] by one of us (B.B.M.). The present paper (which can be read independently) investigates it further, in a manner to be described shortly.

In addition, a second meaning has since been introduced by Frisch and Parisi[6] and by Halsey *et al.*,[7] via a steepest-decent method. The measure (which is normalized to 1) is coarse grained with boxes of size ϵ, yielding a collection $\{p_i(\epsilon)\}_{i=1}^{N(\epsilon)}$ of box measures. The steepest-decent method has led to a multifractal being defined as "a measure for which the partition function $\chi(q,\epsilon)=\sum_{i=1}^{N(\epsilon)}p_i^q(\epsilon)$ scales, for all $-\infty<q<\infty$, like a power law of the form $\chi(q,\epsilon)\sim\epsilon^{\tau(q)}$." For these measures, one obtains a function $f(\alpha)$ by the Legendre transform $\alpha(q)=\partial_q\tau(q)$, and $f(\alpha(q))=\min_q[q\alpha(q)-\tau(q)]$. It always satisfies $f\ge 0$, and the graph of f is shaped like a $\cap$, possibly asymmetric, that is, leaning towards one side.

However, there has recently been much discussion[8–13] of measures such that the partition function diverges faster than a power law, either for small enough negative q values, or for high enough positive q's. For example, Blumenfeld and Aharony,[10] in their study of DLA, have observed that, if coarse-grained probabilities $p_i(\epsilon)$ decay exponentially with ϵ, the function $\tau(q)$ is undefined for all $q<q_{\text{bottom}}=0$. Such measures are "anomalous" from the point of view of Frisch and Parisi and of Halsey *et al.*, and for this reason have been described as being "non-multifractal."[10]

At least two challenges arise thereby. An experimental challenge is to confirm whether or not such an anomaly indeed characterizes diffusion-limited aggregates[14] and other important natural phenomena. A methodological challenge is to provide a conceptual framework for the above-mentioned behavior.

The above "anomaly" is observed in full for resistor networks,[15] and we believe strongly that $q_{\text{bottom}}=0$ is indeed characteristic of DLA and of the dielectric breakdown model (DBM).[16] We also know of an occurrence of $q_{\text{bottom}}=0$ in the study of dynamical systems.[17] However, we think that our experimental arguments concerning DLA are more appropriately described elsewhere.[18] The present paper's goal is, to the contrary, purely methodological. We describe explicitly a class of multiplicative cascades which generate exactly self-similar nonrandom measures, with the properties that $\tau(q)$ fails to be defined for $q<0$ and that the minimal coarse-grained probability decays like a stretched exponential. The fact that these

measures are exactly self-similar makes them multifractals in the more general sense advocated at the beginning of this paper, and makes a detailed investigation possible. When it is necessary to refer to measures for which $\tau(q)$ is defined *for all* q, we shall call them multifractals in a restricted sense, or "restricted multifractals."

The fact that exact renormalizability or self-similarity can be compatible with the failure of the partition function to scale is surprising, but very reassuring, from the point of view of a theoretical study of DLA or DBM. It means that existing approaches[19,20] for the analytical estimation of the multifractal spectrum of DLA and DBM, which are based on an assumption of self-similarity of the harmonic measure, may be extended to include the "anomalies" to be discussed. A clue is implicit in the examples to follow.

The reader may be reassured to know that counterparts of the functions $f(\alpha)$ and $\tau(q)$ continue to be needed in the examples to follow, and that they continue to be cap-convex (like $-x^2$). It also continues to be true that $f(\alpha(q))=\min_q[q\alpha(q)-\tau(q)]$. As to the alternative Legendre transforms, which express both α and f as functions of q, they only apply for those values of q for which the partition function does scale like a power. We already know that, when $q_{\text{bottom}}=0$, the left-hand side ($q<0$) of $\tau(q)$ is undefined. As for $f(\alpha)$, its right side for $\alpha>\alpha(0)$ is degenerate. When $\alpha(0)<\infty$, one has $f(\alpha)=D_0$ for $\alpha>\alpha(0)$. Since only the left-hand side of our $f(\alpha)$ looks as it does in a multifractal in the restricted sense, we refer to our fractal measures as *left-sided.*

While most of the focus has been[9–11] on establishing the existence of a critical point, this paper and closely related ones[5] also focus on the singular behavior of the function $\tau(q)$ ("free-energy") near q_{bottom}. From an analogy with thermodynamics, q_{bottom} is referred to as a critical point. The discontinuity of order n in the $f(\alpha)$ at q_{bottom} is sometimes referred to as an "nth-order phase transition" in $f(\alpha)$. In DLA and DBM, for example, the transition is believed to be first or third order.[9,10,21] Here we show that exponentially decaying probabilities can also lead to second-, higher-order, and smooth (∞-order) transitions, characterized by a new exponent κ.

We also address problems related with the detection of such transitions in measures which are insufficiently sampled. To this end we show how a multiplicative measure can be sampled by a general "random-walk" method. This method is used to make samples of the above left-sided measures, and to study the effect upon $f(\alpha)$ of the fact that, for this family, every finite sample, however large, amounts to undersampling.

Possible faster-than-power-law decay rates of the minimum coarse-grained probability have recently been discussed in connection with DLA.[12] Reference 5 shows that one can generalize our multifractals to include such a behavior.

II. LEFT-SIDEDNESS CAUSED BY EXPONENTIAL DECAY: EXACT RESULTS

A. The measures and their $\tau(q)$

Our measures are supported by the unit interval [0,1] and are the outcome of a deterministic multiplicative cascade process m_β. As usual, the cascade starts by subdividing the unit interval [0,1] into subintervals I_β of length r_β, and giving the βth interval the mass m_β. At the next stage, each of the I_β receives the same treatment, in the sense that it is subdivided into subintervals of size $r_\beta r_{\beta'}$, with respective masses $m_\beta m_{\beta'}$, etc. The theoretical $\tau(q)$ of the resulting measure is known to be given by the "generating equation"

$$Z(q,\tau)=\sum_{\beta=1}^{\infty} m_\beta^q r_\beta^{-\tau(q)}=1 \ . \tag{1}$$

The telling feature of our multifractals, and the key difference with standard examples (such as the binomial measure), is the presence of an infinite base, i.e., of an infinite number of multipliers and reduction factors r_β, namely,

$$m_\beta=2^{-\beta}, \quad r_\beta=|I_\beta|=\beta^{-\lambda}-(\beta+1)^{-\lambda} \ .$$

The intervals I_β are defined as $I_\beta=[(\beta+1)^{-\lambda},\beta^{-\lambda}]$, and $\lambda>0$ is a parameter. We shall say that the generator is $\{r_\beta,m_\beta\}_{\beta=1}^{\infty}$. Motivations for this and other similar choices of generator can be found in Ref. 5.

For our generator, it is easy to show that, for all λ,

$$\tau(q)=\begin{cases}\text{undefined}, & q<0\\ -1, & q=0\\ \tau_\lambda(q), & q>0.\end{cases} \tag{2}$$

This establishes the left-sidedness of this family. We shall say that the critical point is $q_{\text{bottom}}=0$.

To find out about $\alpha(0)$, we observe that $Z(q,\tau)=1$ for $q=0$ and $\tau(0)=-1$. For q to the right of q_{bottom}, it follows that

$$\begin{aligned}Z(q,\tau(q))&\simeq Z(0,-1)+q\frac{\partial}{\partial q}Z(q,\tau(q))\big|_{q=0}\\ &=1+q\frac{\partial}{\partial q}Z(q,\tau(q))\big|_{q=0} \ .\end{aligned}$$

To ensure that $Z(q,\tau(q))=1$, we impose the condition

$$\begin{aligned}0&=\frac{\partial}{\partial q}Z(q,\tau(q))\big|_{q=0}\\ &=-\sum_{\beta=1}^{\infty}2^{-q\beta}r_\beta^{-\tau(q)}\ln(2^\beta r_\beta^{-\alpha(q)})\big|_{q=0}\\ &=-\ln 2\sum_{\beta=1}^{\infty}\beta r_\beta-\alpha(0)\sum_{\beta=1}^{\infty}r_\beta\ln r_\beta \ ,\end{aligned} \tag{3}$$

so $\alpha(0)=(-\ln 2\sum_{\beta=1}^{\infty}\beta r_\beta)/(\sum_{\beta=1}^{\infty}r_\beta\ln r_\beta)$. Using the approximation $r_\beta\simeq\lambda\beta^{-\lambda-1}$ for $\beta\gg1$, and replacing the sums by integrals, we find that $-\sum_{\beta=1}^{\infty}r_\beta\ln r_\beta$ is finite for all $\lambda>0$, while the numerator behaves like $\sum_{\beta=1}^{K}\beta r_\beta\sim K^{1-\lambda}$. We therefore find that

$$\alpha(0)=\begin{cases}\infty, & \lambda\le1\\ \alpha_\lambda(0)<\infty, & \lambda>1.\end{cases} \tag{4}$$

In order to determine the precise behavior of the function $f(\alpha)$ near $\alpha=\alpha(0)$, we solve Eq. (1) near $q=q_{\text{bottom}}=0$. The analysis, which is rather technical, as

seen in the Appendix, yields

$$\tau(q)=-1+\begin{cases} c_1 q+c_2 q^2+\cdots, & \lambda>2 \\ c_1 q+c_2' q^2 \ln q, & \lambda=2 \\ c_1 q+c_\lambda q^\lambda+\cdots, & 1<\lambda<2 \\ c_1' q \ln q+c_1 q, & \lambda=1 \\ c_\lambda q^\lambda, & 0<\lambda<1 \end{cases} \tag{5}$$

where the constants c_1, c_2, etc., depend on λ. This establishes the singular behavior of $\tau(q)$ near $q=q_{\text{bottom}}$. From Eq. (5) it is easy to compute $\alpha(q)$ near $q=q_{\text{bottom}}$ and recover the results in Eq. (4). Inverting this $\alpha(q)$ and eliminating q from the Legendre transform $f(\alpha(q))=q\alpha(q)-\tau(q)$, gives the following asymptotical behavior:

$$f(\alpha)\simeq 1-\begin{cases} c[\alpha_\lambda(0)-\alpha]^\kappa, & \lambda>1, \quad \alpha\nearrow\alpha_\lambda(0) \\ ce^{-c'\alpha}, & \lambda=1, \quad \alpha\to\infty \\ c\alpha^\kappa, & 0<\lambda<1, \quad \alpha\to\infty \end{cases} \tag{6}$$

where c and c' are positive constants which depend on λ and $\kappa=\max\{2,\lambda/(\lambda-1)\}$.

The order of the transition in the $f(\alpha)$ at $q_{\text{bottom}}=0$ is given by the smallest value of n such that $\partial_\alpha^n f(\alpha)|_{\alpha=\alpha_\lambda(0)}\neq 0$. It thus follows that the transition is smooth, i.e., of ∞ order, for $0<\lambda\leq 1$. For $\lambda>1$, the order $n=\kappa$ when κ is integer, and $n=[\kappa]+1$ for κ noninteger. Here $[\kappa]$ is the integer part of κ. Hence the transition is of order 2 for all $\lambda\geq 2$. Then, as $\lambda\searrow 1$, the order of the transition increases continuously and diverges as $(\lambda-1)^{-1}$. It stays infinite for all $0<\lambda\leq 1$.

For $\lambda>1$, which means that $\alpha(0)$ is finite, the left half of $f(\alpha)$ is shaped like the left half of $\cap$ for $\alpha<\alpha(0)$ (see Sec. II B). The right-hand side of $f(\alpha)$ is the horizontal $f=1$, and the order of the discontinuity increases from 2 to ∞, as λ approaches 1 from above. For $\lambda\leq 1$, $\alpha(0)=\infty$, and the right side of $f(\alpha)$ is nonexistent. These behaviors of $f(\alpha)$ are schematically depicted in Fig. 1.

B. An analytical expression for $\alpha_{\min}$

For $q\to\infty$, we know that

$$\tau(q)=\alpha_{\min}q+f(\alpha_{\min}) ,$$

which allows us to rewrite Eq. (1) as

$$\sum_{\beta=1}^{\infty}\exp[-q(A_\beta+\alpha_{\min}B_\beta)-f(\alpha_{\min})B_\beta]=1 , \tag{7}$$

where

$$A_\beta=\ln 2^\beta ,$$

$$B_\beta(\lambda)=\ln[\beta^{-\lambda}-(\beta+1)^{-\lambda}] .$$

In the limit $q\to\infty$, Eq. (7) implies that

$$A_\beta+\alpha_{\min}B_\beta(\lambda)\geq 0, \quad \forall\beta>0 . \tag{8}$$

Now let us define $\alpha_\lambda(\beta)$ by

$$\alpha_\lambda(\beta)=-\frac{A_\beta}{B_\beta(\lambda)} , \tag{9}$$

and α_λ^-

$$\alpha_\lambda^-=\min_{\beta=1,\ldots,\infty}\alpha_\lambda(\beta) . \tag{10}$$

Since $B_\beta(\lambda)<0$ and $A_\beta>0$, $\forall\beta>0$, it is clear that $A_\beta+\alpha_\lambda^- B_\beta(\lambda)>0$ for all values of β such that $\alpha_\lambda(\beta)\neq\alpha_\lambda^-$. Any choice of $\alpha_\lambda^-=\alpha_\lambda(\beta)$, that would not satisfy Eq. (10), would result in violation of Eq. (8) and thus in a divergence of the sum in Eq. (7). Therefore

$$\alpha_{\min}(\lambda)=\alpha_\lambda^-=\min_{\beta=1,\ldots,\infty}-\frac{A_\beta}{B_\beta(\lambda)} . \tag{11}$$

Note that Eq. (11) can be applied to any multiplicatively generated measure whose generating function is of the form

$$\sum_\beta A_\beta^{-q}B_\beta^{-\tau(q)}=1 .$$

One can easily show that $-A_\beta/B_\beta(\lambda)$ has a unique minimum for real values of β. It is reasonable to assume that also after restriction to integer values we find a unique minimum at $\beta=\beta^*$. Equation (7) then reduces to

$$\exp[-f(\alpha_{\min})B_{\beta^*}]=1$$

from which it follows that $f(\alpha_{\min}(\lambda))=0$.

For small values of λ one finds that $\alpha_\lambda^-=\alpha_\lambda(\beta=1)$, and thus that $\alpha_{\min}(\lambda)$ goes to zero as $-\ln(2)/\ln(1-2^{-\lambda})$. On the other hand, for $\lambda\gg 1$, one has that $B_\beta(\lambda)\approx-\lambda\ln\beta$ and $A_\beta=\beta\ln 2$, from which it follows that $\alpha_{\min}(\lambda)\simeq(3\log_3 2)\lambda^{-1}$. So $\alpha_{\min}$ also vanishes for $\lambda\to\infty$. Further implications of $\alpha_{\min}=0$ are discussed in Ref. 5.

The solid curve in Fig. 2 is a numerical solution of Eq. (11). The two discontinuities in the first derivative of this exact curve are due to the fact that for λ less than about 0.8, the minimum in Eq. (11) is determined by the term $\beta=1$, while for λ more than about 1.8 the minimum is determined by $\beta=3$. In between it is $\beta=2$. The boxes are numerical results discussed in Sec. III.

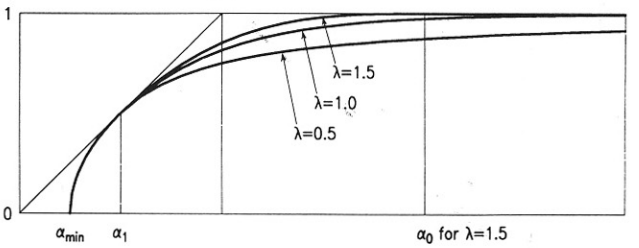

FIG. 1. The left-sided $f(\alpha)$ of the family introduced here [Eq. (6)] can have a finite or infinite $\alpha(0)$. In the finite case, the discontinuity in the $f(\alpha)$ at $\alpha(0)$ can be of any finite order larger than 2. In the infinite case, the transition is smooth and f converges either exponentially or as a power law to its asymptotic value $f=D_0=1$.

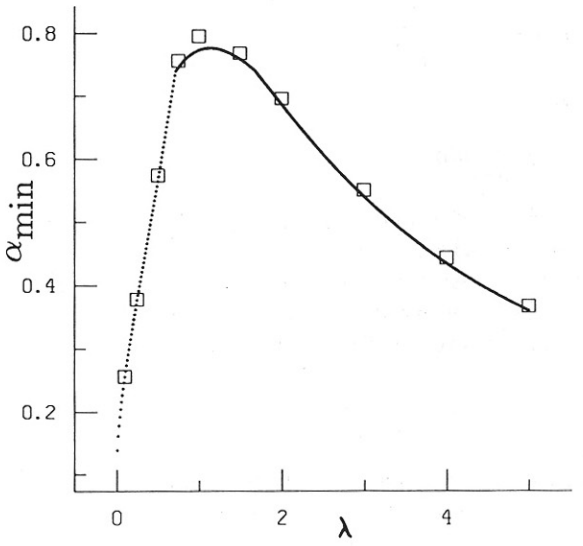

FIG. 2. The solid curve is the exact result for $\alpha_{\min}$, as a function of the parameter λ, parametrizing the family of left-sided multifractals discussed here. The minimal Hölder vanishes both for $\lambda \to 0$ and $\lambda \to \infty$. The boxes are numerical results obtained from $\tau(q)$, solving Eq. (1) using the Newton method.

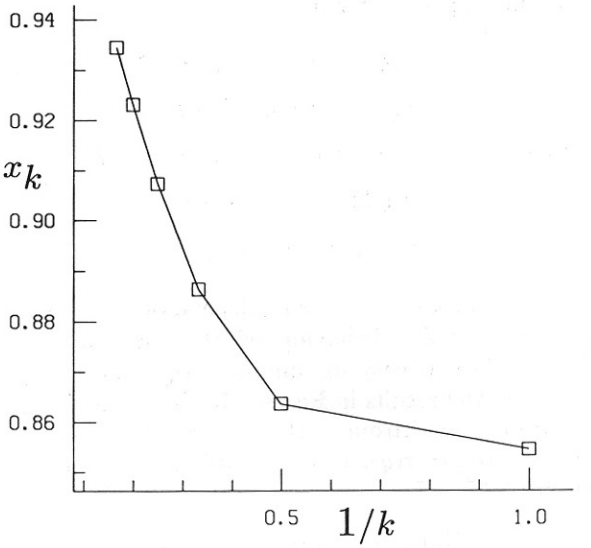

FIG. 4. To study the curvature in the $\lambda=1$ curve in Fig. 3, we plot the local slope $x_k=\log_{10}(\tau_k)-\log_{10}(\tau_{k-1})$ vs $1/k$, where $\tau_k=\tau(10^{-k})$. A simple linear extrapolation yields $x_\infty(\lambda=1)=0.99\pm0.01$, which is in close agreement with the exact result.

III. NUMERICAL SOLUTION OF THE GENERATING EQUATION

The above analysis says nothing of the shape of $f(\alpha)$ between $\alpha_{\min}$ and the asymptotic range. In alternative models, an analytical solution may even be lacking for small q. It is therefore of importance to test numerical solutions against the analytical solution when the latter are known. To this end, we have solved for $\tau(q)$ by Newton's method, that is, using the iteration

$$\tau^n(q)=\tau^{n-1}(q)+\Delta\tau^{n-1} ,$$

where

$$\Delta\tau^{n-1}=[1-Z(q,\tau)]/[\partial_q Z(q,\tau)]\big|_{\tau^{n-1}} .$$

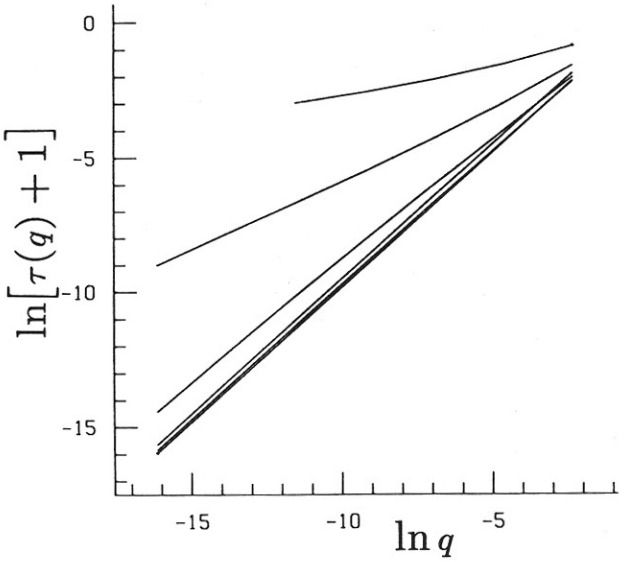

FIG. 3. Plots of the numerically evaluated $\ln[\tau(q)+1]$ versus $\ln q$, for $q=10^{-k}$, $k=1,\ldots,7$, obtained with Newton's method from Eq. (1). For $\ln q=-10$, the values of λ are from top to bottom: $\lambda=0.1$, 0.5, 1, 1.5, 2, and 3.

In Fig. 3 we plot $\ln[\tau(q)+1]$ versus $\ln q$, for $q=10^{-k}$, $k=1,\ldots,7$ and $\lambda=0.1,0.5,1,1.5,2,3$. The slopes of these curves are estimates of the exponent x in $\tau(q)=-1+cq^x$, for $0<q\ll1$. This exponent is related to the exponent λ in Eq. (5), in an obvious way. For $\lambda=0.1$ the above two smallest values of q have not been computed, because of the slow convergence of the sums involved in $Z(q,\tau)$ and $\partial_q Z(q,\tau)$. From the slopes of the lines in Fig. 3, one finds that $x\approx1$ for $\lambda=1.5,2,3$. The case $\lambda=1$ is more difficult to handle: the plot is not quite straight and its curvature becomes apparent in the plot (Fig. 4) of the local slope $\log_{10}[\tau(10^{-k})]-\log_{10}[\tau(10^{-k+1})]$ versus $1/k$. A simple linear extrapolation yields $x(\lambda=1)=0.99\pm0.01$. The above results, and those obtained from a similar analysis for $\lambda=0.1$ and 0.5, agree very well with the exact results in Eq. (5).

Taking the Legendre transform of the $\tau(q)$ obtained by the above method for $0.0005<q<102$, we find the $f(\alpha)$ shown in Fig. 5 for $\lambda=1$ and 0.5. As expected, the convergence of $f(\alpha)$ to $f=1$ is much faster for $\lambda=1$ than for $\lambda=0.5$, while the convergence of $\alpha(q)$ to infinity, as $q\to0$, is faster for $\lambda=0.5$. The results for $\alpha(q=102)$ are also shown as boxes in Fig. 2. The slight discrepancies are due to the finiteness of the value of q used.

It is clear from these examples that, in certain cases, the asymptotics of $f(\alpha)$, or the value of the critical exponent x, depend on values of q that are either extremely close to 0, or extremely large.

IV. SAMPLING OF MULTIPLICATIVELY GENERATED MEASURES BY A RANDOM WALK

The measures underlying physical processes are usually estimated by some sampling procedure. In dynamical

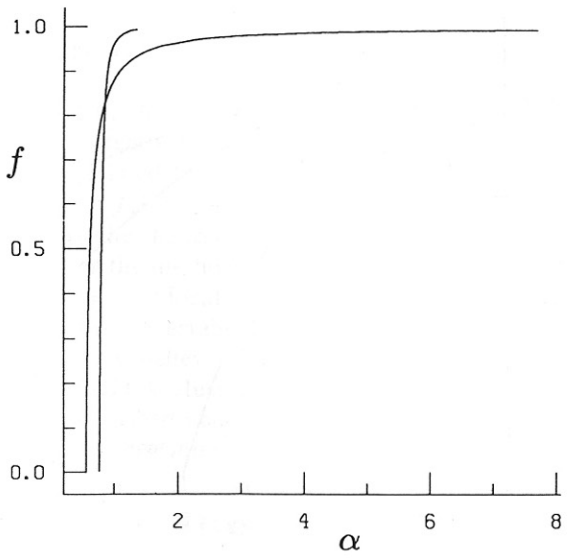

FIG. 5. Numerical evaluation of the theoretical $f(\alpha)$ for $\lambda=0.5$ (curve 1) and for $\lambda=1$ (curve 2). Both were obtained by Legendre transforms of numerical solutions of Eq. (1), using Newton's method.

systems,[22] one can iterate the map in order to find the measure on the attactor. The harmonic measure on DLA clusters can be found by sending many random walkers and keeping track of how often the different growth sites are being visited.[23] It is important, therefore, to understand how the existence of a critical point and critical behavior can be established in the presence of finite sampling. As a first step, we now describe a method that can serve to sample one of our left-sided measures up to a prescribed precision $\delta=2^{-N}$.

The sampling is done by subdividing the interval [0,1] into 2^N bins of size δ. The measure μ_j in bin $[j\delta,(j+1)\delta]$, $j=1,\ldots,1/\delta$, is the result of a particular multiplicative history $\{\beta_1,\ldots,\beta_n\}$ resulting in a box of size $\epsilon_n=\prod_{i=0}^{n} r_{\beta_i}\approx\delta$ and is given by $\mu_j=\prod_{i=1}^{n} m_{\beta_i}=\prod_{i=1}^{n} 2^{-\beta_i}$. Note that when a measure is constructed on a regular lattice of base r, one has $\epsilon_n=r^n$ independently of the position of the bin. In the present case, however, the r_β are not equal, hence n depends on the position of the bin. We can therefore sample the measure by generating random sequences $\{\beta_1,\ldots,\beta_n\}$, where β is chosen according to the probability distribution $\text{prob}(\beta)=m_\beta=2^{-\beta}$ and n is the finite value such that $\epsilon_n\approx\delta$. The bin visited by this particular sequence is $[\Delta,\Delta+\epsilon_n]$, where $\Delta=\sum_{j=1}^{n}\epsilon_{j-1}(\beta_j+1)^{-\lambda}$ and $\epsilon_0\equiv 1$.

It is good to think of this process in terms of a random walk with $-\ln\mu$ along the x axis and $-\ln\epsilon$ along the y axis. At time 0, let our random walker start at the origin. Then the walker selects at each step among an infinite number of possible next steps, indexed by $\beta=1,2,\ldots$, each with probability $2^{-\beta}$. When β has been chosen, the walker will jump by $\beta\ln 2$ in the x direction and by $-\ln r_\beta$ in the y direction, and so on. To reach the desired precision δ, the walker has to proceed until it crosses the line $y=-\ln\delta$. Since the jumps in the vertical direction are not equal, the required number of steps will be strongly dependent on the choice of jumps.

Given M walks, denote by ϕ_j the number of times the bin j has been visited by a walk. Then $M^{-1}\phi_j$ is an estimate of the measure μ_j of this particular bin. To assess the sampling accuracy, note that the bin of size δ with the smallest measure is clearly $[0,\delta]\in[0,1]$. This measure equals 2^{-z}, with $z=\delta^{-1/\lambda}-1$. Therefore, our family of left-sided measures is such that, as a function of the coarse-graining box size ϵ, the smallest probability decays like a *stretched exponential*

$$p_{\min}(\epsilon)\sim\exp(-\epsilon^{-1/\lambda}\ln 2)\ .$$

This implies that a precision δ requires at least $M(\delta,\lambda)=2^z$ walks. For example, for $\lambda=1,0.5,1.5$, one finds $M(2^{-8},1)\approx 10^{76}$, $M(2^{-5},1)\approx 10^{9}$, $M(2^{-4},1)\approx 35\,000$, $M(2^{-3},0.5)\approx 10^{19}$, and $M(2^{-8},1.5)\approx 10^{11}$. Figure 6 shows the estimated measure $(M^{-1}\phi_j)$ of a sample of the measure for $\lambda=1$, obtained with $M=4\times 10^8$ walks and $\delta=2^{-15}$. Similar samples were constructed for $\lambda=0.5$ and 1.5.

Estimating $f(\alpha)$

We will now briefly discuss what happens if one attempts to estimate the $f(\alpha)$ of this sampled measure, using a method[24] that is closely related to those of Refs. 6 and 7. We expect to find problems with these methods, due to the divergence of negative moments. One might also expect additional problems, due to the fact that our measures are generated with unequal reduction factors, while the partition function involves a covering with boxes of equal size.

Figure 7 plots $\alpha(q,\epsilon)=\chi^{-1}(q,\epsilon)\sum_{i=1}^{N(\epsilon)} p_i^q(\epsilon)\ln p_i(\epsilon)$ versus $\ln\epsilon$ for $\lambda=1$, where the quantities χ and p_i are as defined in the Introduction. This graph's slope, according to Ref. 24, is $\alpha(q)$. As expected, the plot for $q=-0.5$ clearly shows that only boxes of size $\epsilon\geq 2^{-4}$ are meaningful. That is, since we have sampled the measure with $M(2^{-4},1)<M<M(2^{-5},1)$ walks, we expect that

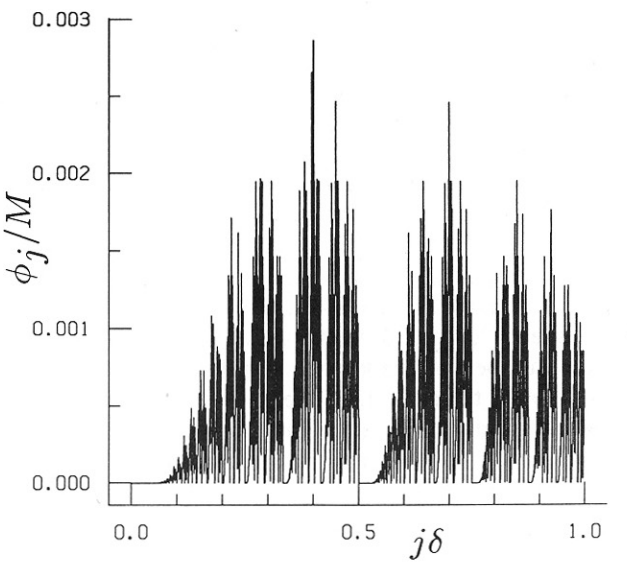

FIG. 6. The $\lambda=1$ measure, sampled with $M=4\times 10^8$ walks. The size of the bins used to make this histogram is $\delta=2^{-11}$.

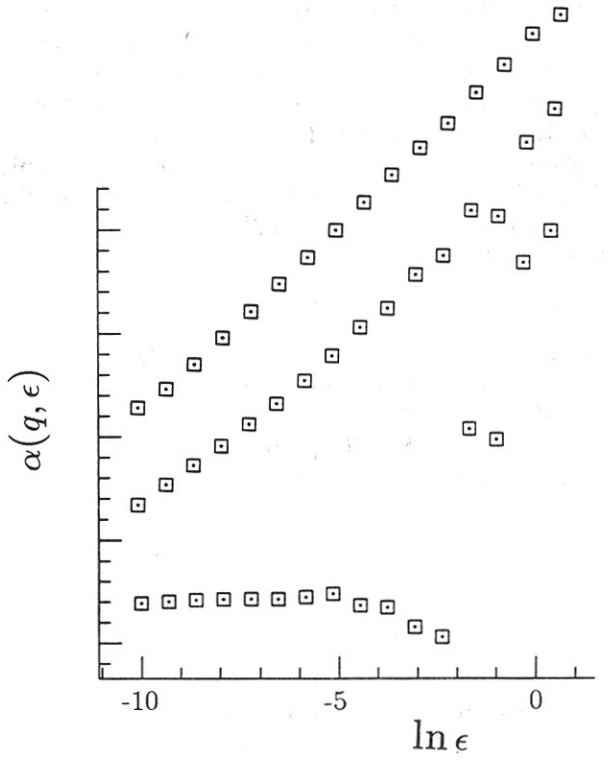

FIG. 7. From top to bottom, the slopes of these curves are supposed to be $\alpha(q)$, $q=1,0,-0.5$. There is no scale on the vertical axis, because it is different for each curve. The idea is to show the effects of undersampling and of divergent moments on these plots of $\alpha(q,\epsilon)$ vs $\ln\epsilon$.

there is at least one bin of size 2^{-5} which has been visited only once, and therefore has measure M^{-1}. But then the same is true for all $\epsilon<2^{-5}$. Because M^{-1} dominates in the partition function for $q\ll 0$, we expect a crossover to slope zero in Fig. 7 for $\epsilon<2^{-5}$. Clearly, the same happens at smaller box sizes for larger values of q.

The systematic curvature in the $q=0$ plot for $\epsilon\geq 2^{-4}$ implies that the quantity $\alpha_\epsilon(q)\equiv[\alpha(q,\epsilon)-\alpha(q,\epsilon/2)]/\ln 2$, which can be called an "effective value of $\alpha(q)$," increases with decreasing ϵ. To better examine the consequences of this monotonicity, we have computed $f(\alpha)$ for $1<q<15$, by means of a least-squares fit through all the box sizes $2^{-14}\leq\epsilon\leq 2^{-1}$. Figure 8 represents this portion of the $f(\alpha)$ curve by dots. For $-15<q<1$, we computed an effective $f_\epsilon(\alpha)$ curve using $\alpha_\epsilon(q)$ and $f_\epsilon(q)$. The function $f_\epsilon(q)$ is defined in the same way as $\alpha_\epsilon(q)$, using[24] $f(q,\epsilon)=q\alpha(q,\epsilon)-\tau(q,\epsilon)$, where $\tau(q,\epsilon)=\ln\chi(q,\epsilon)$. The values of ϵ giving the right-hand portions of the $f(\alpha)$ in Fig. 8 are 2^{-k}, $k=2,3,4$. This plot suggests that for an infinite number of walks, the whole $q<0$ part of the $f_\epsilon(\alpha)$ moves towards 1, while at the same time being pushed towards $\alpha=\infty$, as $\alpha_\epsilon(q=0)$ diverges to infinity.[5] This result would confirm the prediction in Ref. 10.

In Fig. 9, we show the most asymptotic results ($k=4$) we could get with the above number of walks for $\lambda=1$, together with the much more accurate results obtained from solving Eq. (1) with the Newton method and then doing a Legendre transform. Because of the truncation

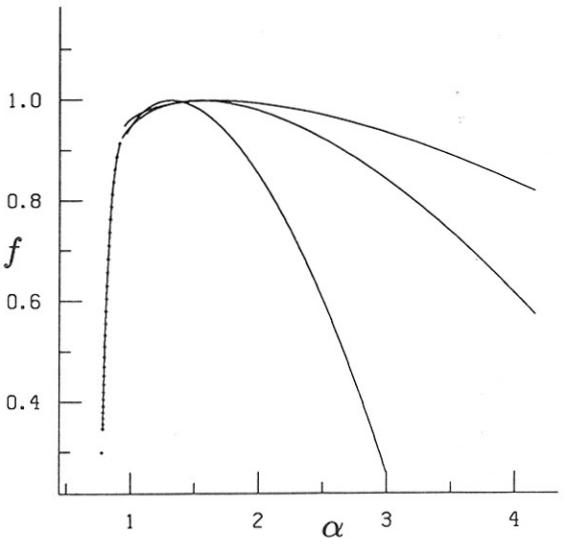

FIG. 8. A method based on the partition function is used to estimate the $f(\alpha)$ of the sample showed in Fig. 6. Because of curvature in the log-log plots determining the exponents for $q<1$ (see Fig. 7), we plot an effective $f_\epsilon(\alpha)$ curve for $\epsilon=2^{-k}$, $k=2,3,4$, for this range of q. The dotted curve, which corresponds to $1\leq q\leq 15$, was determined using the slope through all box sizes.

at $\alpha=2.5$, the above encountered problems concerning $q<1$, i.e., $\alpha\gtrsim 1$, are less apparent in this figure. For $\alpha<1$, we expect the number of walks to be sufficient, hence are inclined to take seriously the close agreement between different methods for evaluating $f(\alpha)$. In this range, even though the measure was generated with mul-

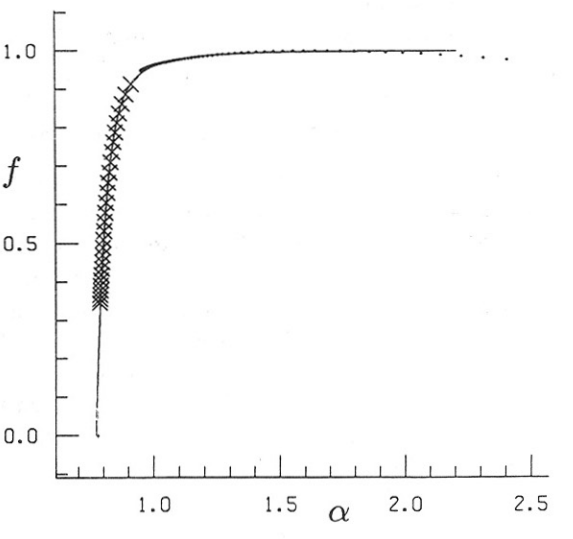

FIG. 9. This figure concerns $\lambda=1$, and combines results from the generating equation and from the partition function. The solid line is the result for $\lambda=1$ shown in Fig. 5. The crosses are equal to the dotted part of Fig. 8. The dotted portion equals the $k=4$ portion of Fig. 8. In the range $q>1$, i.e., $\alpha<1$, the good agreement suggests that multiplicative measures generated with unequal reduction factors can be analyzed by the usual multifractal formalism based on a covering with equal-sized boxes. the problems encountered for small q, as discussed in the text, do not show on this figure because of the truncation at $\alpha=2.5$.

tipliers m_β with unequal r_β, one may be able to use a partition function based on a covering with boxes of equal size.

For $q \leq 0$, the curvature in the $\alpha(q,\epsilon)$ plots confirms what we already know: neither the exponents $\alpha(q)$ nor $f(q)$ are defined for $q<0$. Nevertheless, one can define an effective $f_\epsilon(\alpha)$ curve, which in the limit $\epsilon \to 0$, seems to tend to the theoretical result. This therefore provides support for the methods used in Refs. 9 and 10, where the dependence of "local" exponents on the cluster size L was invoked in establishing phase transitions in DLA. We therefore believe that high-precision data on large DBM and DLA clusters, combined with the method of analysis described above, can shed more light on the nature of the transition in these models.

V. DISCUSSION AND SUMMARY

The above described critical behavior will in general occur for any measure for which $\tau(q)=\tau(q_{\text{bottom}}) + c_1 q + c_2 q^2 + c_x q^x + O(q^3)$, with x being a noninteger critical exponent characterizing the singular behavior of τ near the critical point q_{bottom}. For the family of measures parametrized by $0<\lambda<\infty$, considered here, we showed that the exponent is $x=\lambda$. The order n of the transition in the $f(\alpha)$ was shown to be equal to $n=[\kappa]+1$ for $x>1$ and $n=\infty$ for $x \leq 1$, where $\kappa=\max[2, x/(x-1)]$. Thus the order of the transition in $f(\alpha)$ undergoes two transitions as a function of λ. At $\lambda=2$ there is a first-order transition, while at $\lambda=1$ there is a "smooth" transition from finite to infinite order, characterized by $n \sim (\lambda-1)^{-1}$.

In this family of measures, the smallest probability decays like a *stretched exponential* $p_{\min}(\epsilon) \sim \exp(-c\epsilon^{-s})$, as a function of the coarse-graining box size ϵ, with $s=1/\lambda$. This establishes a one-to-one relation $s=1/x$, between the stretched exponential decay of the smallest probability and the exponent x, and thus also between s and the order of the transition in the $f(\alpha)$. We believe that this relation holds in general. This would imply that the lower bound $s>D-1$, suggested in Ref. 19, where $D \approx 1.7$ is the fractal dimension of DLA clusters, leaves open the possibility for a transition of any order in the $f(\alpha)$ of DLA.

Other rules for the decays of the minimal probability are possible. For example, $p_{\min}(\epsilon) \sim \exp[-c(-\ln\epsilon)^{-y}]$, has recently[12] been suggested for DLA. Reference 5 shows that this rule is also compatible with self-similarity of the measure.

We have shown that the existence of exponentially decaying probabilities does not necessarily imply that a measure fails to be self-similar. This was achieved by an explicit construction and detailed investigation of exactly self-similar (or renormalizable) measures having this property. This result implies that phenomena such as DLA, for which the smallest growth probabilities are believed to decay faster than power law, may still be compatible with the concept of multifractality, as long as this concept is taken in its original more general sense.[1] The price to pay is that the partition function, as a tool to estimate $f(\alpha)$, fails for certain ranges of values of q. In the multiplicatively generated left-sided multifractal measures discussed in this paper, the exponent $\tau(q)$ is undefined for $q<0$. We show this can give rise to second- and higher-order phase transitions in $f(\alpha)$. These transitions are characterized by a critical exponent κ, which (at least in the measures considered in this paper) is determined by the exponent characterizing the stretched exponential decay of the smallest probability. We have also discussed how these transition could manifest themselves in experimental data, and thus how they can be found in real systems.

ACKNOWLEDGMENTS

We would like to thank Don Coppersmith of IBM Yorktown for his extremely valuable contribution. The bulk of the Appendix is due to him. We also would like to thank Craig Kolb of Yale for considerable help with programming and graphics. This research has been financially supported in part by the U.S. Office of Naval Research, Grant No. N00014-88-K0217.

APPENDIX

We solve Eq. (1) for all λ in the limit of small positive values of q, i.e., $q \downarrow 0$. Let $\delta=q \ln 2$, $q>2$, $q>0$ and write $\tau(q)=-1+\varepsilon$. Since the nontrivial behavior of the measures studied here is caused by the behavior of the multipliers m_β for large values of β, we can use the approximation $r_\beta \simeq \lambda \beta^{-\lambda-1}$. Thus we can replace the reduction factors by $r_\beta=\beta^{-\lambda-1}/\zeta(\lambda+1)$, where the Riemann zeta function $\zeta(x)=\sum_{j=1}^{\infty} j^{-x}$ is introduced to ensure that the slightly changed lengths r_β add to 1. The original problem, Eq. (1), then becomes

$$\sum_{\beta=1}^{\infty} e^{-\delta\beta} r_\beta^{1-\varepsilon} = \zeta(\lambda+1) .$$

If we define $s_\beta=(1-e^{-\delta\beta})r_\beta$ and $t_\beta=e^{-\delta\beta}(r_\beta^{1-\varepsilon}-r_\beta)$, the above equation becomes

$$\sum_{\beta=1}^{\infty} (s_\beta - t_\beta) = 0 . \tag{A1}$$

This sum is split into three parts, namely,

$$\Sigma(1) \equiv \sum_{\beta<1/\delta} s_\beta , \tag{A2}$$

$$\Sigma(2) \equiv \sum_{\beta>1/\delta} s_\beta , \tag{A3}$$

$$\Sigma(3) \equiv \sum_{\beta=1}^{\infty} e^{-\delta\beta} (\beta^{\varepsilon(\lambda+1)}-1)/\beta^{\lambda+1} , \tag{A4}$$

so that Eq. (A1) becomes

$$\Sigma(1)+\Sigma(2)-\Sigma(3)=0 . \tag{A5}$$

For $\Sigma(1)$ we find

$$\Sigma(1) = \sum_{\beta<1/\delta} \frac{1}{\beta^{\lambda+1}} \left[\sum_{n=1}^{\infty} (-1)^{n+1} \frac{(\delta\beta)^n}{n!} \right] .$$

Since this double sum is absolutely convergent we can rearrange terms to find for $\lambda \neq 1, 2, \ldots$, that

$$\Sigma(1)=\sum_{n=1}^{\infty}[(-1)^{n+1}/n!]\delta^n\sum_{\beta<1/\delta}\beta^{n-1-\lambda} \tag{A6}$$

$$=\sum_{n=1}^{\infty}\frac{(-1)^{n+1}}{n!}\delta^n\left[\frac{\beta^{n-\lambda}}{n-\lambda}\Bigg|_1^{1/\delta}\right] \tag{A7}$$

$$=\sum_{n=1}^{\infty}\frac{(-1)^{n+1}}{n!}\left[\frac{\delta^{\lambda-n}}{n-\lambda}+C_n+\cdots\right] \tag{A8}$$

$$=\delta^{\lambda}\left[\sum_{n=1}^{\infty}\frac{(-1)^{n+1}}{n!(n-\lambda)}\right]+\sum_{n=1}^{\infty}\frac{(-1)^{n+1}}{n!}\delta^n C_n+\cdots, \tag{A9}$$

where the ellipsis represents lower-order terms. Note that for $1<\lambda<2$ the term in large parentheses (A9) lies in the range $(-\infty,-2.8]$. It follows that

$$\Sigma(1)\approx\begin{cases}c\delta+c''\delta^2+\cdots, & \lambda>2\\ c\delta+c'\delta^2\ln(1/\delta)+c'''\delta^2, & \lambda=2\\ c\delta+c_1\delta^{\lambda}+\cdots, & 1<\lambda<2\\ c\delta\ln(1/\delta)+c'\delta, & \lambda=1\\ c\delta^{\lambda}+c'\delta+\cdots, & 0<\lambda<1,\end{cases} \tag{A10}$$

with $c_1<0$. The results for $\lambda=1$ and 2 follow from Eq. (A6). Since $0.63<c_2'\equiv[1-\exp(-\delta\beta)]<1$ we can write $\Sigma(2)$ as

$$\Sigma(2)=c_2'\sum_{\beta>1/\delta}\beta^{-\lambda-1}=\frac{c_2'}{\lambda}\delta^{\lambda}+\cdots\sim c_3\delta^{\lambda}\cdots,$$

where $c_2=c_2'/\lambda$ and $|c_1|>|c_2|$ if $1<\lambda<2$. By Taylor's theorem with remainder

$$\Sigma(3)=\sum_{\beta=1}^{\infty}\frac{e^{-\delta\beta}}{\beta^{\lambda+1}}\left[\epsilon(\lambda+1)\ln\beta+O\left[\frac{\varepsilon^2}{2}(\lambda+1)^2\ln^2(\beta)\beta^{\epsilon(\lambda+1)}\right]\right].$$

The first term has the upper bound

$$T(1)\equiv\sum_{\beta=1}^{\infty}\frac{e^{-\delta\beta}}{\beta^{\lambda+1}}\varepsilon(\lambda+1)\ln\beta<\sum_{\beta=1}^{\infty}(\ln\beta/\beta^{\lambda+1})\varepsilon(\lambda+1)\equiv c_3\varepsilon$$

and the lower bound

$$T(1)>\sum_{\beta<1/\delta}\frac{(1-\delta\beta)\ln\beta}{\beta^{\lambda+1}}\varepsilon(\lambda+1) \tag{A11}$$

$$=\sum_{\beta<1/\delta}\frac{\ln\beta}{\beta^{\lambda+1}}\varepsilon(\lambda+1)-\delta\sum_{\beta<1/\delta}\frac{\ln\beta}{\beta^{\lambda}}\varepsilon(\lambda+1) \tag{A12}$$

$$=c_3\varepsilon-O(\delta^{\lambda}\ln(1/\delta)\varepsilon)-\begin{cases}O(\delta\varepsilon), & \lambda>1\\ O(\delta\varepsilon\ln^2(1/\delta)), & \lambda=1\\ O(\delta^{\lambda}\varepsilon\ln(1/\delta)), & \lambda<1.\end{cases} \tag{A13}$$

The expression $\Sigma(3)-T(1)$ is of the order $O(\varepsilon^2)$, as long as $(1-\varepsilon)(1+\lambda)>1$, so that

$$\Sigma(3)\simeq c_3\varepsilon+O(\varepsilon^2)+O(\varepsilon\delta^{\lambda}\ln(1/\delta))+\begin{cases}O(\delta\varepsilon), & \lambda>1\\ O(\delta\varepsilon\ln^2(1/\delta)), & \lambda=1\\ O(\delta^{\lambda}\varepsilon\ln(1/\delta)), & \lambda<1.\end{cases}$$

Equation (A5) then yields

$$\varepsilon=\begin{cases}c\delta+c''\delta^2+\cdots, & \lambda>2\\ c\delta+c''\delta^2\ln(1/\delta), & \lambda=2\\ c\delta+c''\delta^{\lambda}+\cdots, & 1<\lambda<2\\ c\delta\ln(1/\delta)+c''\delta, & \lambda=1\\ c\delta^{\lambda}+O(\delta)+O(\delta^{2\lambda}\ln(1/\delta)), & 0<\lambda<1,\end{cases}$$

as announced in the body of this paper.

*Present address: Education Center for Information Processing, Tohoku University, Sendai 980, Japan.

[1]B. B. Mandelbrot, J. Fluid Mech. **62**, 331 (1974).

[2]B. B. Mandelbrot, in *Statistical Physics 13, Proceedings of the Union of Pure and Applied Physics International Conference, Haifa, 1977,* edited by D. Cabib, C. G. Kuiper, and I. Riess (Hilger, Bristol, 1987), p. 225.

[3]B. B. Mandelbrot, *The Fractal Geometry of Nature* (Freeman, New York, 1982).

[4]B. B. Mandelbrot, in Ref. 1 and other earlier papers are to be reprinted in B. B. Mandelbrot, *Fractals and Multifractals: Noise, Turbulence and Galaxies Selecta* (Springer, New York, in press), Vol. 1.

[5]B. B. Mandelbrot, Physica A **168**, 95 (1990).

[6]U. Frisch and G. Parisi, in *Turbulence and Predictability of Geophysical Flows and Climate Dynamics,* Proceedings of the International School of Physics "Enrico Fermi," edited by M. Ghil, R. Benzi, and G. Parisi (North-Holland, New York, 1985), p. 84.

[7]T. C. Halsey, M. H. Jensen, L. P. Kadanoff, I. Procaccia, and B. I. Shraiman, Phys. Rev. A **33**, 1141 (1986).

[8]B. B. Mandelbrot, Pure. Appl. Geophys. **131**, 5 (1989); in *Random Fluctuations and Pattern Growth,* Vol. 157 of *NATO Advanced Study Institute, Series E: Applied Science,* edited by H. E. Stanley and N. Ostrowsky (Kluwer Academic, Dordrecht, 1988), pp. 345–360.

[9]J. Lee and H. E. Stanley, Phys. Rev. Lett. **61**, 2945 (1988).

[10]R. Blumenfeld and A. Aharony, Phys. Rev. Lett. **62**, 2977 (1989).

[11]B. B. Mandelbrot, in *Fractals' Physical Origins and Properties,* Proceedings of the International School of Physics "Ettore Majorana," Erice, Italy, 1988, edited by L. Pietronero (Plenum, New York, 1989), p. 3.

[12]S. Schwarzer, J. Lee, A. Bunde, S. Havlin, H. E. Roman, and H. E. Stanley, Phys. Rev. Lett. **65**, 603 (1990).

[13]See, e.g., A. Aharony and J. Feder, Physica D **38**, 1 (1989).

[14]T. A. Witten and L. M. Sander, Phys. Rev. Lett. **47**, 1400 (1981).

[15]R. Blumenfeld, Y. Meir, A. Aharony, and A. B. Harris, Phys. Rev. B **35**, 3524 (1987).

[16]L. Niemeyer, L. Pietronero, and H. J. Wiesmann, Phys. Rev. Lett. **52**, 1033 (1984).

[17]B. B. Mandelbrot, in *Chaos in Australia,* edited by G. Brown (World Scientific, Singapore, 1990).

[18]B. B. Mandelbrot and C. J. G. Evertsz, Nature (to be published).

[19]T. Nagatani, J. Phys. A **20**, L381 (1987); Phys. Rev. A **36**, 5812 (1987); J. Phys. A **20**, L641 (1987); **20**, 6135 (1987).

[20]L. Pietronero, A. Erzan, and C. J. G. Evertsz, Phys. Rev. Lett. **61**, 861 (1988); Physica **151A**, 207 (1988).

[21]P. Trunfio and P. Alström, Phys. Rev. B **41**, 896 (1990).

[22]M. H. Jensen, L. P. Kadanoff, A. Libchaber, I. Procaccia, and J. Stavans, Phys. Rev. Lett. **55**, 2798 (1975).

[23]P. Meakin, in *Phase Transitions and Critical Phenomena,* edited by C. Domb and J. Lebowitz (Academic, New York, 1988), Vol. 12, p. 335.

[24]A. Chhabra and R. V. Jensen, Phys. Rev. Lett. **62**, 1327 (1989).